Cell Cycle 14:20, 3261–3269; October 15, 2015; Published with license by Taylor & Francis Group, LLC

New distinct compartments in the G_2 phase of the cell cycle defined by the levels of γH2AX.

Idun Dale Rein[1], Caroline Stokke[2,3], Marwa Jalal[4], June H Myklebust[5,6], Sebastian Patzke[1], and Trond Stokke[1,*]

[1]Group for Molecular Radiation Biology; Department of Radiation Biology; The Norwegian Radium Hospital; Oslo, Norway; [2]The Intervention Centre; Oslo University Hospital; Oslo, Norway; [3]Faculty of Health Sciences; Oslo and Akershus University College of Applied Sciences; Oslo, Norway; [4]The Francis Crick Institute; London, UK; [5]Group for Lymphoma and Lymphocyte Biology; Department of Cancer Immunology; The Norwegian Radium Hospital; Oslo, Norway; [6]Centre for Cancer Biomedicine; University of Oslo; Oslo, Norway

Keywords: DNA repair, G_2 cell cycle phase, ionizing radiation, PARP inhibition, γH2AX

Induction of DNA double strand breaks leads to phosphorylation and focus-formation of H2AX. However, foci of phosphorylated H2AX (γH2AX) appear during DNA replication also in the absence of exogenously applied injury. We measured the amount and the number of foci of γH2AX in different phases of the cell cycle by flow cytometry, sorting and microscopy in 4 malignant B-lymphocyte cell lines. There were no detectable γH2AX and no γH2AX-foci in G_1 cells in exponentially growing cells and cells treated with PARP inhibitor (PARPi) for 24 h to create damage and reduce DNA repair. The amount of γH2AX increased immediately upon S phase entry, and about 10 and 30 γH2AX foci were found in mid-S phase control and PARPi-treated cells, respectively. The γH2AX-labeled damage caused by DNA replication was not fully repaired before entry into G_2. Intriguingly, G_2 cells populated a continuous distribution of γH2AX levels, from cells with a high content of γH2AX and the same number of foci as S phase cells (termed "G_2H" compartment), to cells that there were almost negative and had about 2 foci (termed "G_2L" compartment). EdU-labeling of S phase cells revealed that G_2H was directly populated from S phase, while G_2L was populated from G_2H, but in control cells also directly from S phase. The length of G_2H in particular increased after PARPi treatment, compatible with longer DNA-repair times. Our results show that cells repair replication-induced damage in G_2H, and enter mitosis after a 2–3 h delay in G_2L.

Introduction

The cell cycle of mammalian somatic cells contains 4 well-defined, non-overlapping compartments; G_1, S (DNA replication), G_2 and mitosis (M), in addition to the actual process of cell division (cytokinesis). The G_1 phase varies greatly in length, from hours to years, and the important decision of whether the cell shall proceed through a new round in the cell cycle or not is taken in G_1, specifically at the so-called "restriction point",[1] reviewed by Blagosklonny and Pardee.[2] Passage through the restriction point requires both the presence of appropriate growth factors, and lack of growth inhibitory factors. However, S phase entry may also be blocked after DNA damage, e.g. after ionizing radiation or treatment with genotoxic drugs.[3,4] The processes taking place during G_2 are less well known, but e.g., disentangling of sister chromosomes may require time before the chromosomes can condense,[5] marking the onset of mitosis.[6] There may also be other time-consuming biochemical processes and restructuring required for entry into M. Although somatic mammalian cells do not regulate cell proliferation in G_2, there is a DNA damage checkpoint in this phase, serving a similar purpose as the one in G_1.[7,8] Although the length of G_2 is typically much shorter and more homogeneous than that of G_1 in cells not treated with genotoxic agents, it still varies from 2–7 hours within the same culture for the cell lines employed in this work (see also [9,10]). This somewhat argues against the idea that untreated cells go through a strict set of processes in G_2, which would be expected to take about the same time in each cell.

Lesions in DNA, particularly double-strand brakes (DSBs), initiate an array of events, including DNA repair, cell cycle arrest in G_1 and G_2, and apoptosis if repair is not successful. However, DNA damage may be the result of non-faithful DNA replication, which may also happen in the absence of external injury. Indeed, ATR is activated during DNA replication in untreated, exponentially growing cells, indicating that DNA damage may be induced during an unperturbed S phase.[11,12] Serine 139 on histone H2AX is phosphorylated in the vicinity of DSBs, these sites can be visualized as nuclear foci after staining with antibodies against the phosphoprotein (γH2AX). Several research groups have reported that S phase cells in control, untreated, cultures of both

*Correspondence to: Trond Stokke; Email: tstokke@rr-research.no
Submitted: 05/20/2015; Revised: 08/18/2015; Accepted: 08/22/2015
http://dx.doi.org/10.1080/15384101.2015.1087617

transformed and immortalized cells have such foci[13,14] (reviewed in [15,16]), showing that damage is induced during DNA replication, also in the absence of DNA damaging agents. In contrast, G_1 control cells have undetectable levels of γH2AX. Mitotic cells show varying levels of γH2AX, but the distribution is diffuse rather than focal, and has been suggested not to be associated with DNA damage.[17,18] It is possible that the levels of DNA damage carried over from S phase to G_2 varies from cell to cell, thus requiring different times in G_2 for DNA repair. To our knowledge, there have been no studies addressing the levels of γH2AX in G_2.

In this work we have studied γH2AX in the G_2 phase by flow cytometry and microscopy. We show that individual cells are entering G_2 with various levels of γH2AX, and that they spend variable amounts of time in a compartment in G_2 defined by high γH2AX levels and many foci. This compartment was termed "G_2H;" the "H" refers to high γH2AX levels. After having left this compartment, the cells enter a compartment termed "G_2L" (low γH2AX), more homogeneous in length than G_2H, before they enter mitosis. We thus define 2 entirely new compartments in G_2, and explain how different "shapes" of the cell cycle-resolved content of γH2AX may reflect differences in fidelity of DNA replication/repair between different cell types and lines.

Results

Heterogeneity of γH2AX levels in G2 in control and PARP inhibitor treated cells

Four exponentially growing malignant B-lymphocyte cell lines were studied for cell cycle phase-dependent phosphorylation of H2AX in *interphase* cells (**Fig. 1**). Comparison with samples stained without the primary γH2AX antibody (staining control) showed that the G_1 cells had little, if any γH2AX (**Fig. S1**). γH2AX levels increased immediately upon S phase entry and remained high throughout S. γH2AX levels in control S cells were lowest in Reh, and increasingly higher in U698, Granta-519 and JVM-2. Some G_2 cells had high levels of γH2AX (termed "G_2H," see arrows in **Fig. 1** and **Fig. S1**), while others had lower levels down to almost negative (termed "G_2L"), resulting in a broader γH2AX distribution in this phase. The cell cycle-resolved γH2AX expression pattern was similar in primary (normal) B lymphocytes stimulated to enter the cell cycle (**Fig. S2**). The heterogeneity in γH2AX levels in G_2 was assessed by the "robust coefficient of variation" (rCV), which was significantly higher than the rCV for mid-S phase cells for all cell lines (data not shown). After treatment with 3 μM of the PARP inhibitor Olaparib (PARPi) for 24 h to create damage and inhibit DNA repair,[19] γH2AX in S phase cells was increased relative to the corresponding control, while G_1 cells still had no γH2AX (**Fig. 1**). γH2AX also increased in G_2 cells after PARPi treatment. (See accompanying article in this issue for γH2AX levels in S and G_2 cells with different concentrations of PARPi). The rCV values for G_2 compared to S were significantly higher also after PARPi treatment. Control and PARPi-treated mitotic cells had a high content of γH2AX in the cells studied here (**Fig. 2A**). In contrast to PARPi treatment, irradiation with 4 Gy X-rays 1 h before harvest resulted in an increase in γH2AX in all cell cycle interphases (**Fig. 2A**).

To see how the variable levels of γH2AX in G_2 phase related to DNA damage, the cell cycle-resolved numbers of γH2AX foci were determined in sorted cells from distinct cell cycle phases (sort gates shown in **Fig. S3**), followed by microscopic evaluation. Most G_1 cells had no foci, with some cells displaying 1 focus (**Fig. 2B**), which was also the case after PARPi treatment for 24 h. Mid-S phase cells in control cultures had 10±5 (Reh; mean±SD) and 12±6 (U698) foci, in agreement with the high γH2AX content measured by flow cytometry. PARPi treatment increased focus numbers in mid-S phase cells to 29±11 foci in Reh and 32±10 foci in U698 cells, respectively. γH2AX focus numbers thus increased 2.9 and 2.6 fold upon PARPi treatment in Reh and U698 cells, while the corresponding increase in γH2AX-associated fluorescence by flow cytometry was 3.3 and 2.3 fold (background corrected). Together, these results indicated that replication damage-associated (focal) γH2AX fluorescence was reliably measured by the total intensity in *interphase* cells. In contrast, control mitotic Reh and U698 cells, with high γH2AX intensities, had only 1 focus on average. PARPi treatment for 24 h increased the number of foci to 2 in mitotic Reh cells, but mitotic U698 cells still had 1 focus (**Fig. 2B**). Thus, the diffuse staining in mitotic cells accounted for most of the total γH2AX-associated fluorescence (not shown). The broader distributions observed for the γH2AX-associated fluorescence of G_2 cells by flow cytometry showed that the content of γH2AX in G_2 was more heterogeneous than in S (**Figs. 1, 2A**). We therefore sorted G_2 cells with high (G_2H) and low (G_2L) γH2AX-associated fluorescence to reveal possible differences in focus counts between these 2 compartments (see **Fig. S3** for sort gates). The G_2 cells with high γH2AX content (G_2H) had many foci (10±5 and 16±7 for control Reh and U698 cells, respectively), similar to the S phase cells (**Fig. 2B**), indicating that these cells had similar DNA damage levels. In contrast, the G_2L cells had few foci (3±2 and 2±2 for Reh and U698, respectively). Focus numbers in the 2 G_2 compartments increased after PARPi treatment, most significantly for the G_2H cells. Hence, G_2H and G_2L are well-defined compartments in G_2, although the lack of a clear bimodal distribution indicated a continuous distribution of γH2AX. The lack of consistent bimodal distributions precluded a straight-forward assessment of the fractions of cells in the G_2H and G_2L compartments. In contrast to the heterogeneity seen for PARPi treated G_2 cells, focus counts were homogeneously increased in G_1, S and G_2 cells 1 h after irradiation with 4 Gy (**Fig. 2B**), in agreement with the homogeneously enhanced γH2AX-associated fluorescence in all cell cycle interphases measured by flow cytometry (**Fig. 2A**).

The order of G_2H and G_2L

Non-irradiated cells entered mitosis continuously, also in the presence of PARPi, although at a lower rate than in the control samples (**see later**). Entry into mitosis is known to be prevented by the presence of DSBs, which can be signaled by the presence of γH2AX foci. As mitotic cells had only 1–2 foci, it seems likely

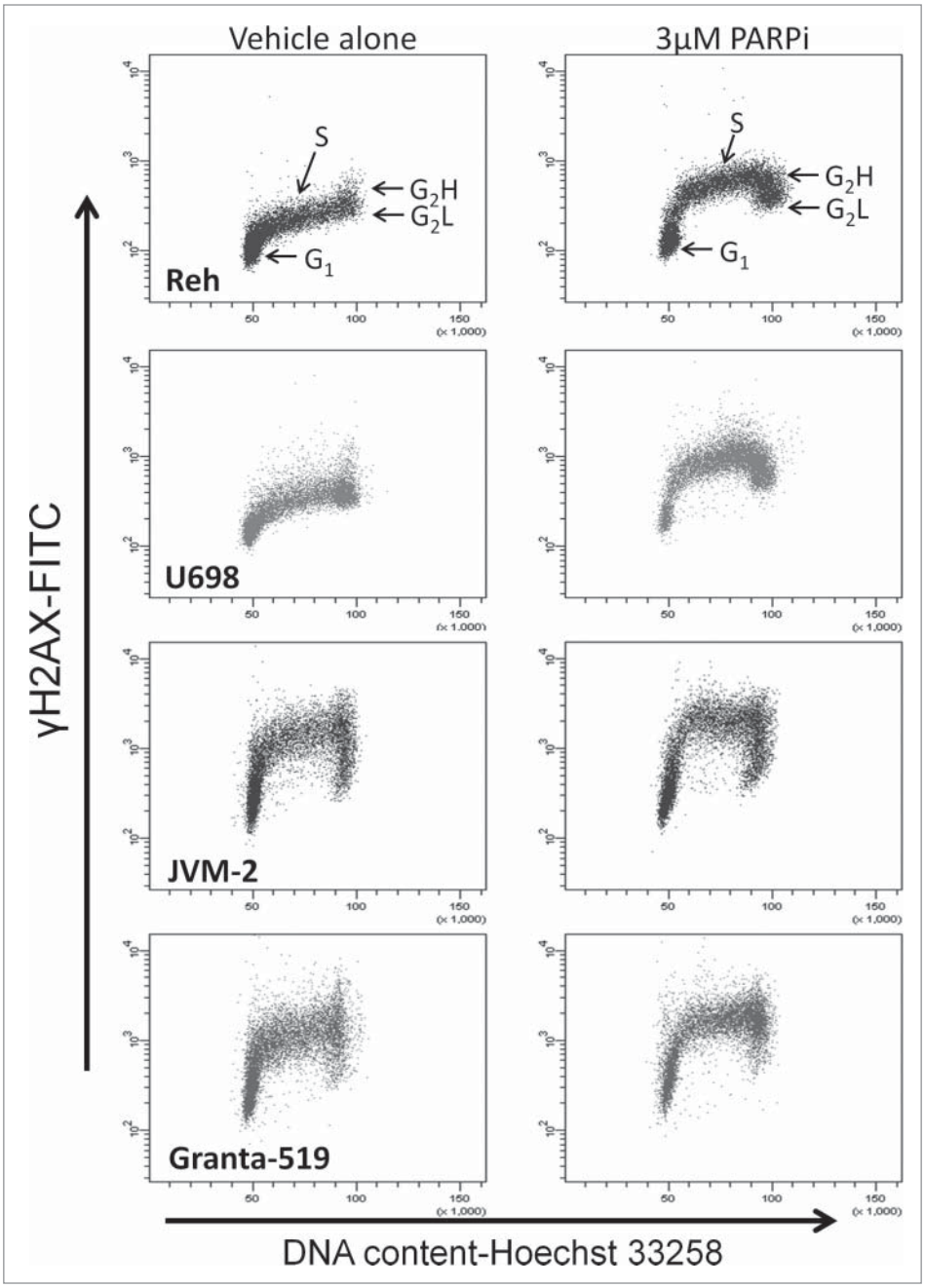

Figure 1. Cell cycle-resolved phosphorylation of H2AX in interphase control and PARPi-treated cells. Cells were grown for 24 h in the absence (left panels), or presence of 3μM the PARPi Olaparib (right panels). They were thereafter fixed and stained for γH2AX, pS10H3, apoptosis, and DNA content and measured by flow cytometry. Aggregates of cells and apoptotic cells (few at this time point, see the accompanying article in this issue), as well as mitotic cells were removed before displaying interphase cells. (See Fig. S4 in the accompanying article in this issue for details.) **Fig. 2A** shows the position of mitotic cells in the cytograms.

that the cells are entering mitosis with a low number of γH2AX foci, possibly from G_2L. To this end, we studied in which order cells proceeded through the 2 compartments in G_2, G_2H and G_2L, by pulse-labeling S phase cells with EdU and chasing them (experimental strategy shown in **Fig. S3**). Data corrected for the spillover of S phase cells are shown in **Fig. 3** (raw data are shown in **Fig. S4**). The G_2H compartment was populated directly from S phase, as the fraction of EdU^+ G_2H cells was increased after 1 h. The entry of EdU-labeled cells into the G_2L compartment always lagged entry into G_2H, with lower initial increases than the corresponding ones for G_2H. The fractions of EdU^+ G_2L cells after 1 h were close to zero in the presence of PARPi, indicating that G_2L was populated exclusively via another compartment (G_2H) under those conditions. Mitosis was populated after both G_2 compartments, and eventually EdU^+ cells entered the next G_1. The plateau levels reached after 8 h for control G_2H and M cells were about 80% (i.e. lower than the theoretical 100%, which may have been caused by a less than ideal separation between the EdU^- and EdU^+ populations). However, the fractions of EdU^+ control cells in the G_2L compartment consistently flattened out at lower levels compared to G_2H and M, particularly pronounced for JVM-2 cells (**Fig. 3**, experimental data). Hence, these results suggest the presence of a subpopulation of G_2L cells that is not leaving the compartment within the time frame of the experiment, and is thus not populating M, possible due to delayed cell death. Cell cycle traverse was slower in the presence of PARPi, and plateau levels reached after 24 h were about 60%. These levels were lower than for control cells, which may be explained by lower DNA replication rates and less intense EdU-labeling. However, plateau levels were similar for G_2H, G_2L, and M, indicating that all cells entering G_2L (from G_2H) proceed to M within the time frame of the experiment.

The duration of the G_2H and G_2L compartments

We further simulated the time evolution of population of the different phases and compartments with EdU^+ cells to extract durations. A similar strategy has been employed to study the duration of G_2 plus M.[9,10] If the duration of G_2H had been constant (T), the fraction of EdU^+ cells in this compartment should have increased linearly with time with a slope proportional to 1/T (an example is shown in **Fig. S5A**). It was evident from the experimental data in **Fig. 3** that a model with constant duration of G_2H could not fit the data in any case. A

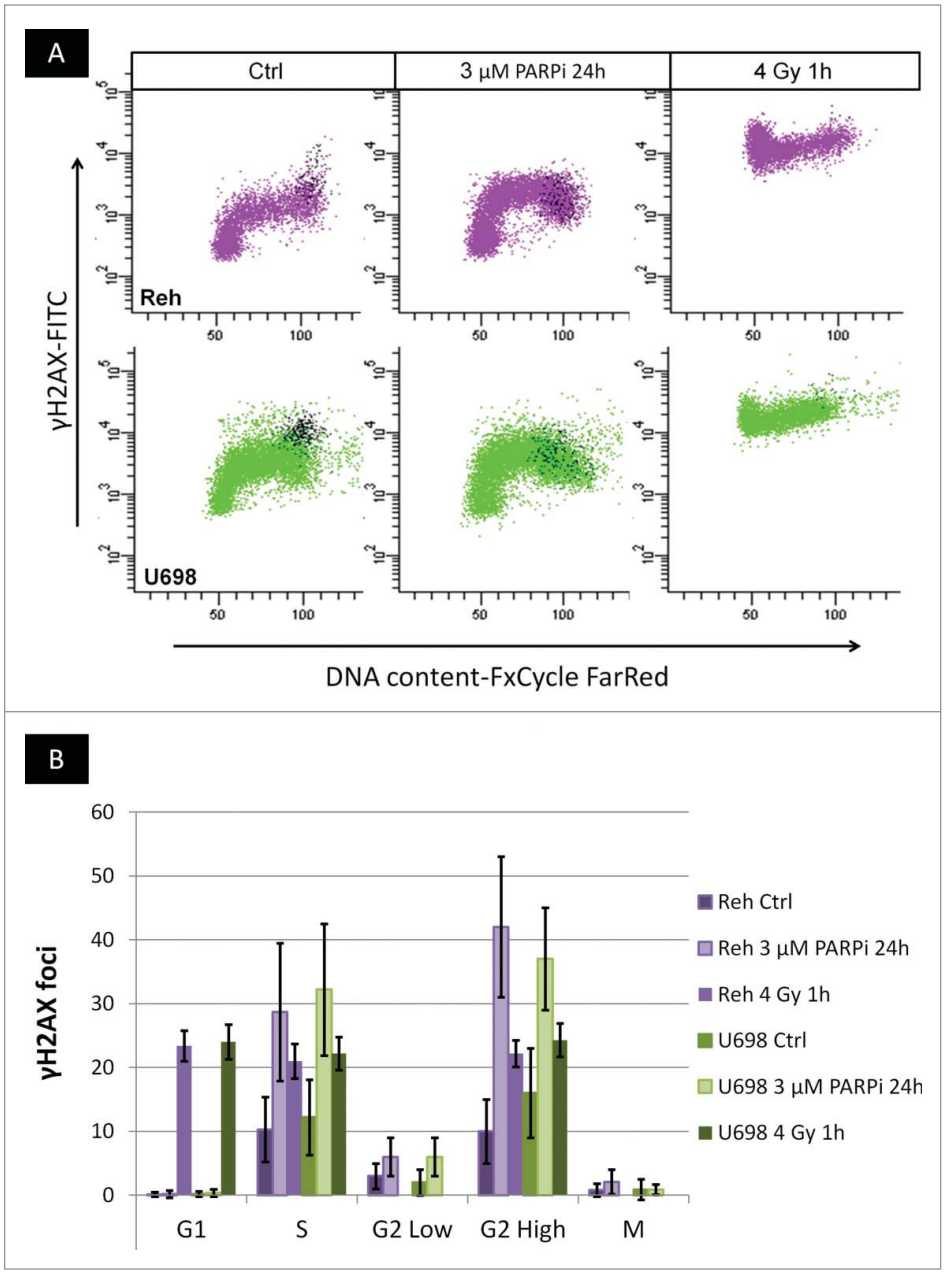

Figure 2. Cell cycle-resolved γH2AX levels and number of γH2AX foci. (**A**) Reh (upper panels) and U698 cells (lower panels) were grown for 24 h in the absence (Ctrl) or presence of Olaparib (3μM PARPi 24 h), or they were irradiated with 4 Gy 1 h before harvest. Cells were fixed and stained for γH2AX, pS10H3, apoptosis, and DNA content and measured by flow cytometry. Aggregates of cells and apoptotic cells were removed before displaying interphase cells (colored dots) and mitotic cells (black dots). (**B**) Cells stained as under (**A**) were sorted according to the scheme in **Fig. S3**, and analyzed for the number of γH2AX foci. There were no mitotic cells and no cells in G_2L in cultures harvested 1 h after 4 Gy IR, and results for irradiated cells are given for G_1, S and G_2H. The plot shows mean ± SD.

model was therefore employed where we allowed for sequential movement from S into G_2H, allowed to vary in length from cell to cell, and further into G_2L before entering M (see Materials and Methods). First we assumed that the flux of cells from S phase into G_2H and further into G_2L and M was the same for the different residence times in G_2H ("flat" distribution, i.e., f(T) = constant; an example is shown in **Fig. S5B**). The time dependency of EdU^+ cells in G_2H of control cells could be reasonably fitted with flat distributions for all 3 cell lines, 0.5–7, 0.5–7.5 and 0.5–6.5 h for Reh, U698 and JVM-2, respectively (simulation curves in **Fig. 3**). However, the data for G_2L and M were not fitted, irrespective of the durations employed for the latter 2 compartments (**Fig. S5B**). Since some cells may enter G_2L directly, i.e. G_2H has zero duration, f(0) was allowed to take non-zero values. Notice that the time course of EdU^+ cells in G_2H will be determined by f(T>0) only. In contrast, the time course of EdU^+ cells in G_2L and M will be affected if a fraction of the cells enter G_2L directly (f(0)>0). The data for G_2L and M at early times were better fitted with this approach, but the time evolutions of EdU^+ cells in G_2L and M at the later times were not fitted employing the "flat" distribution model (**Fig. S5C**). This, and the lower plateau levels in control cells observed for G_2L compared to G_2H and M, indicated that the cells with the longest duration of G_2H did not leave G_2L to enter M within the time frame of the experiment.

We therefore also allowed for variable weighting of the flux of cells out of the compartments with different residence times in G_2H. Mathematically, this was done by allowing f(T) to vary within the time interval found to fit G_2H (see Materials and Methods and **Sup. File**), thus obtaining simulations for G_2L and M. In the case of control cells, good fit was obtained if the distribution of cells entering M through G_2L had a skewed distribution with higher amplitudes toward the lower residence times in G_2H (simulation curves in **Fig. 3**). To fit the G_2L plateau levels of control cells at 8 h, a long lifetime component was added (G_2L: >8 h, not entering M), representing cells that, by implication, were recruited from a skewed distribution with higher amplitudes toward longer residence times in G_2H (**Table 1**).

We considered possible sources of error in these calculations. The gating, and sorting, of mitotic cells was based on pS10H3 staining, which results in clear bimodal peaks and good separation between the pS10H3-positive and -negative cells. Microscopy revealed that there were almost no interphase cells in the

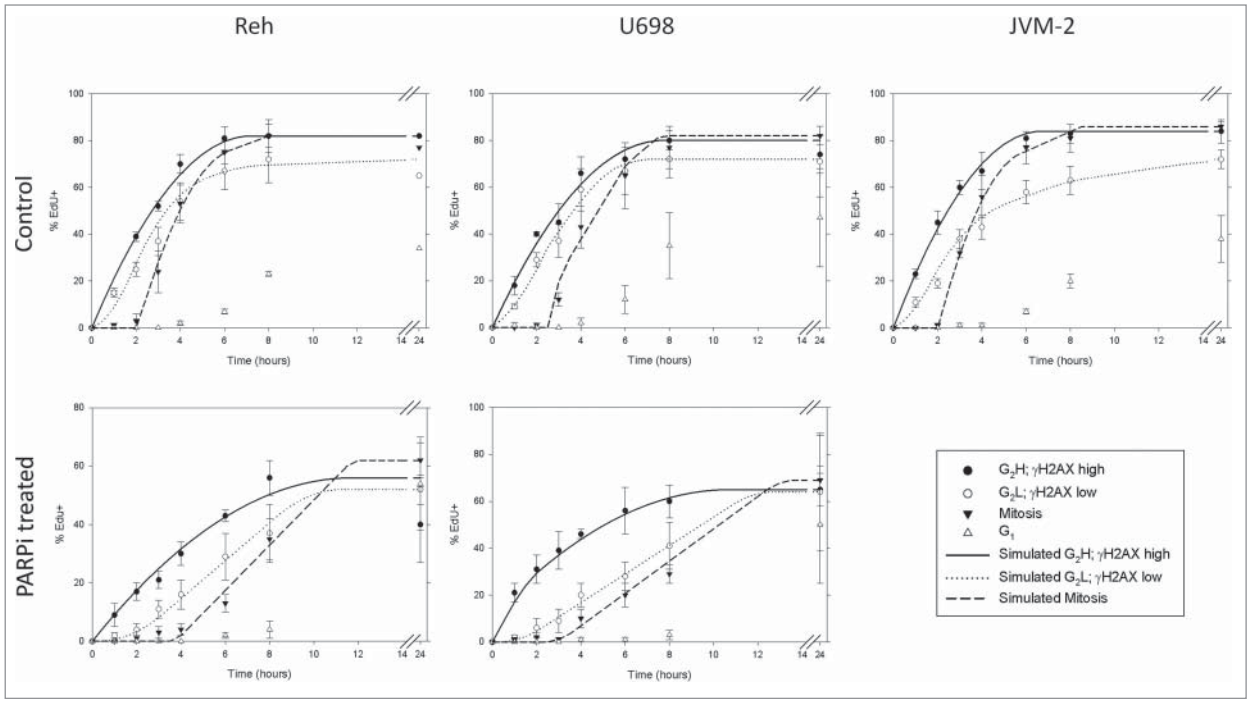

Figure 3. Fraction of EdU^+ cells as a function of time after pulse-labeling. Control cells, or cells treated with the PARP inhibitor Olaparib (3μM) for 24h were pulse-labeled for 15 minutes and chased for the indicated amounts of time. Cells were fixed and stained for γH2AX, pS10H3, EdU, apoptosis, and DNA content and measured by flow cytometry. Aggregates of cells were removed before gating the EdU histograms as shown in **Fig. S3**. Data were corrected for the spillover of (EdU^+) S phase cells into the regions used as gates for the cells in G_2H, G_2L, M, and G_1 (see "Materials and Methods"). The raw data are shown in **Fig. S4**. The lines show the simulated fractions of EdU^+ cells employing a model that involved the sequential entry of cells into a compartment (G_2H) with a variable length, and thereafter into 2 compartments with fixed durations (G_2L followed by mitosis). (See "Materials and Methods." The program was written in Excel and is provided as supplementary file "H2AXCellCycleSupfile.xlsm".) The data for G_2H control cells were simulated employing flat distributions, 0.5–7, 0.5–7.5 and 0.5–6.5 h for Reh, U698 and JVM-2, respectively. The G_2L and M data of control cells were fitted assuming skewed distributions toward the shorter residence times in G_2H (**Table 1**). The G_2L cells with a long lifetime were assumed, by implication, to be recruited from the cells with the longest duration of G_2H, these fractions were calculated from the plateau levels at 8 h and are thus not simulated *per se*. The data for G_2L and M of PARPi treated cells were simulated with flat distributions in G_2H, 0.5–8 h and 0.5–10.5 h for Reh and U698, respectively. To fit the G_2H data of PARPi treated cells, we added G_2H components not entering G_2L and M of 8.5–11.5 h for Reh and 1–2 h for U698. The parameters employed to obtain the best fit to the data are given in **Table 1**.

$pS10H3^+$ fraction. However, the gating/sorting of the G_2H and G_2L populations was more difficult, since the γH2AX distributions were more or less continuous. Although there was a pronounced difference between the *mean* focus counts in G_2H and G_2L (**Fig. 2B**), the distributions were overlapping, particularly for control Reh and U698 cells (**Fig. S6**), where the dynamics of γH2AX staining was lower than in JVM-2 control cells, and lower as compared to PARPi treated cells. This indicated that some G_2L cells may have been included in the G_2H gate, and vice versa. This will result in EdU^+ curves for G_2H and G_2L approaching each other. This "gating" error suggests that we should interpret the data for control Reh and U698 cells with caution. Additionally, we have not performed simulations varying all parameters, and there may be other sets of values fitting the experimental data than the ones given in **Table 1**.

Simulation of the time evolution of EdU^+ cells was simpler after PARPi treatment. Cell cycle progression was slower, and plateau levels for EdU+ cells were assumed to be reached 24 h after EdU-labeling. G_2L and M were well fitted with flat distributions in G_2H, 0.5–8 h and 0.5–10.5 h for Reh and U698, respectively (**Table 1**). However, these distributions did not fit G_2H in either case, and we added G_2H components not entering G_2L and M of 8.5–11.5 h for Reh and 1–2 h for U698. These latter may be cells dying directly from G_2H, possibly as a result of high levels of DNA damage.

Discussion

The length of the G_2 phase of the cell cycle varies by several-fold among individual cells in the same culture. Novel findings of this work include that cells in G_2 phase have heterogeneous levels of γH2AX, ranging from the high levels observed in S phase cells (G_2H) down to almost negative (G_2L). The heterogeneity is partially caused by different levels of replication-induced DNA damage in the cells leaving S phase, but is modulated by repair, such that the G_2H cells are eventually entering G_2L. The G_2L compartment lasts for 2–3 h, and entry into mitosis occurs exclusively from G_2L. Thus, the variation in G_2

Table 1. The durations of cell cycle phases and subcompartments from simulation of the time evolution of the fraction EdU^+ cells.

	G_2H (hours)	G_2L (hours)	Mitosis (hours)
Reh control	17%: 0 →	2 →	0.5
	81%: 0.5–5.5[1] →	2 →	0.5
	2%[2]: 1–7 →	>8 → Delayed death	
Reh PARPi treated	70%: 0.5–8 →	3 →	1.5
	30%: 8.5–11.5 → Apoptosis		
U698 control	28%: 0 →	2.5 →	0.5
	69%: 0.5–4.5[1] →	2.5 →	0.5
	3%[2]: 3.5–7.5 →	>8 → Delayed death	
U698 PARPi treated	57%: 0.5–10.5 →	2 →	1.5
	43%: 1–2 → Necrosis		
JVM-2 control	21%: 0 →	2 →	0.5
	74%: 0.5–6.5[1] →	2 →	0.5
	5%[2]: 1–6.5 →	>8 → Delayed death	

The fluxes of cells from S phase into the compartments are given by the percentages. The flux equals the fraction of cells with that residence time divided by the residence time. (See "Materials and Methods.") A zero value for G_2H means that this fraction of cells entered G_2L directly (f(0)>0). When a range of times is given, the distribution of fluxes used in the simulations was flat, except for:

[1]The distribution was skewed with higher amplitudes toward the lower times.

[2]These fractions were calculated from the plateau levels (at 8 h for control cells) using the residence times in the table for the G_2L cells entering M, and 10 h for the long-lived G_2L cells not entering M. The latter figure is a low estimate, leading to some overestimation of the corresponding flux figures.

length is explained by the variation in G_2H, i.e., the time it takes to repair DNA damage to a level below the threshold for entry into mitosis.

Cell cycle-resolved phosphorylation of H2AX in unperturbed cell cycles has been studied in several articles (reviewed in [15,16]). G_1 cells have been reported to be negative, which was also the case for the 4 malignant B-lymphocyte cell lines studied here, even after 24 h treatment with the PARP inhibitor Olaparib (PARPi). H2AX was phosphorylated in control cells upon S phase entry, and the levels of γH2AX remained high and almost constant through this phase. Hence, if damage is created continuously in S phase, some DNA repair must take place to balance the newly created damage. PARPi treatment increased the S phase levels further. However, the 4 cell lines had different levels of γH2AX in S phase, which will be discussed in the context of γH2AX in G_2 later. Importantly, proliferating primary normal B-lymphocytes showed a similar cell cycle-resolved γH2AX phosphorylation pattern as the malignant cell lines, so the DNA damage created was not necessarily the result of oncogene-induced replication stress. Mitotic cells had high levels of γH2AX, but the localization was diffuse rather than focal, suggesting that γH2AX is not associated with DNA damage under these conditions.[17,18] We have earlier shown that γH2AX foci may be found in mitotic cells after lower doses of ionizing radiation,[20] but in those experiments we had to sort the cells for microscopic evaluation of focus numbers to avoid the high diffuse background in mitotic cells in flow cytometry experiments. The correlation between total γH2AX levels measured by flow cytometry and number of foci as measured by microscopic inspection argues that DNA damage-associated phosphorylation of H2AX after replicative stress can be reliably measured by flow cytometry in interphase cells.

In contrast to PARPi treatment, ionizing radiation induced H2AX phosphorylation to a similar degree in all interphases. An important difference between these treatments is that there is a complete and lasting arrest in G_2 following 4 Gy IR in these malignant lymphocyte cell lines ([21] and unpublished results). We have measured the decay of γH2AX in G_2 with time after irradiation with 4 Gy (unpublished); the levels never decreased to those of control cells. Thus, inability to repair the damage completely may explain why irradiated (≥4 Gy) lymphocytes never enter mitosis, but eventually die by apoptosis (Reh, Granta519), or necrosis (U698, JVM-2). PARPi-treated cells, on the other hand, continue through the cell cycle (Fig. 3 and Fig. S2 in the accompanying article in this issue). Also, the intensities measured by flow cytometry after IR (**Fig. 2A**) were higher than expected from the γH2AX focus counts (**Fig. 2B**, compare with control and PARPi treated cells), indicating that the γH2AX foci observed after IR are larger than the replication-induced foci. Our unpublished results have shown that the diameter of replication-induced γH2AX foci is 0.7–1.0 μm, while IR-induced foci have a diameter of about 1.2 μm. The nature of the damage and damage detection/repair may thus be different after IR compared to replication-induced DNA damage.

γH2AX levels in G_2 cells in control or PARPi treated cultures were more heterogeneous than in the other phases, with levels ranging from the high levels observed in S phase, down to almost negative. As the cells entered mitosis with up to 2 foci, it is suggested that cells may enter G_2 with high γH2AX levels (G_2H) from S phase, repair the (remaining) replication-induced γH2AX-associated DNA damage, thus entering G_2L, and eventually mitosis (**Fig. 4**). If the damage levels of (some) cells exiting S phase are low, which was observed in control samples, they may enter G_2L and thereafter M directly. Evidence for this hypothesis came from tracking EdU-labeled cells through G_2 and mitosis (**Fig. 3**). The G_2H compartment was always populated directly from S phase, but G_2L was only partially populated directly from S phase (in control cultures), or exclusively recruited through G_2H (in PARPi treated cultures). Mitosis was always populated indirectly through G_2L. Importantly, mitotic

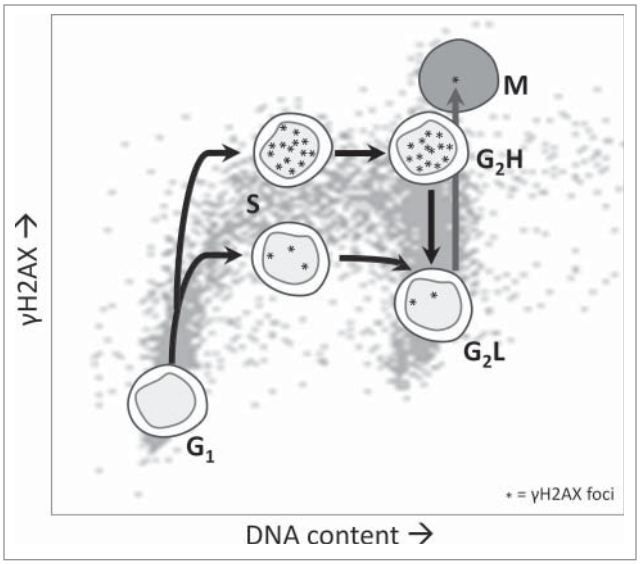

Figure 4. A model for the transition of cells through G_2 according to the amount of DNA damage created during S phase. DNA replicating control cells have different levels of γH2AX, from low levels corresponding to a few foci, up to levels corresponding to about 15 foci. The S phase cells with low levels of γH2AX enter G_2L directly and then proceed to M after about 2 h. The ones with high levels of γH2AX-associated damage enter G_2H, repair the damage, thus entering G_2L and eventually M. The mitotic cell in the figure has been given a gray shade to illustrate the diffuse background of γH2AX staining in this phase. After inhibition of PARP for 24 h, the damage in cells entering G_2 is increased, and no cells enter G_2L directly.

cells also exited from mitosis, with somewhat increased transit times in the presence of PARPi. However, not all cells in G_2H may enter G_2L, as was observed for PARPi-treated Reh and U698 cells (**Table 1**). We may speculate that the cells leaving S phase with the highest levels of DNA damage after PARPi treatment die in G_2H. The long lifetime of dying Reh cells may reflect that they tend to die by apoptosis, while the corresponding short lifetime of dying U698 cells may reflect that they die by necrosis after PARPi treatment (see the accompanying paper in this issue). Likewise, not all cells that enter G_2L may continue into M. Examples of this are provided by control cultures, where we found (a low fraction of) long-lived G_2L cells that did not enter mitosis. Since the cells entering M was recruited from a distribution that was skewed toward the shorter residence times, it is implied that the long-lived cells in G_2L originate from the compartment with the longest residence times (highest γH2AX content) in G_2H. It is possible that these cells repair the γH2AX-associated damage, but that there are other types of DNA damage present preventing entry into M. We show in Fig. 7 in the accompanying article in this issue that PARPi treatment may lead to tri- and tetra-radial chromosomes, telomeric fusions or chromatid breaks, particularly pronounced in the presence of ATM inhibitor. Such chromosome aberrations may be caused by non-faithful non-homologous end joining, leading to inter-chromosomal translocations. DSBs and other γH2AX-labeled damage may thus be repaired under those circumstances, but it is not known whether inappropriate recombination events can trigger the G_2-M checkpoint.

Finally, our results explain why the cell cycle-resolved expression of γH2AX varies between cell lines. The steady state levels of damage during S phase is determined by the fidelity of DNA replication, as well as the rate of DNA repair. If the damage created during S phase is large, most cells enter G_2 with a high content of γH2AX. Under these circumstances, the G_2 cells must repair extensively before entry into G_2L and mitosis, and the DNA versus γH2AX cytograms will have an inverted "U"-like appearance (**Fig. 1**; PARPi treated cells and to some degree JVM-2 and Granta519 control cells). However, if the cells leave S phase with less damage, a significant fraction of them enter G_2L directly. The heterogeneity in γH2AX levels in G_2 is thus less pronounced, and less visible in the cytograms (**Fig. 1**; control Reh and U698 cells).

In conclusion, we have shown that cells enter G_2 with varying levels of γH2AX, depending on the amount of DNA damage carried over from S phase. The ones with high levels of damage spend time in a compartment termed G_2H until the damage levels are low enough for the cells to enter mitosis through a compartment termed G_2L. The cells that enter G_2 with low levels of damage, corresponding to 1–2 γH2AX foci, enter G_2L directly and thereafter mitosis 2–3 hours later.

Materials and methods

Cell culture and treatment

Four malignant lymphocyte cell lines Reh, U698, JVM-2 and Granta-519 were grown as previously described.[21] Cells were pulse-labeled with 10 μM EdU (Life Technologies) for 10 minutes 24 hours after addition of 3 μM PARP inhibitor (Olaparib/AZD2281, Selleck Chemicals) or vehicle. Cells were washed after the EdU pulse and reseeded in 50/50 conditioned media containing the same amount of PARP inhibitor/vehicle. Cells were irradiated with an X-ray generator (Faxitron CP160) at 160 kV, 6.3 mA (dose rate 1 Gy/min). Peripheral blood B-lymphocytes were isolated from anonymous, healthy donors at The Blood Bank in Oslo, after informed consent and with approval from regional authorities (REK S-03280). B cells were isolated using positive selection with CD19 Dynabeads (Life technologies), according to the manufacturer's description. B cells were cultured for 96 h, reseeded at 0.6×10^6 cells/ml in X-VIVO 15 (PAA) supplemented with 20 ng/mL rhu IL-21 (eBioscience) and CD40L (Alexis Biochemicals, Enzo Life Sciences), and grown for another 24 h. The CD40L was pre-incubated with enhancer for ligand (final concentrations of 0.25 ug/mL and 1 ug/mL for CD40L and enhancer, respectively), before addition to the culture medium.

Antibodies and dyes

The EdU Click-iT® Alexa Fluor® 647 Kit (Life Technologies) was used following the manufacturer's instructions. Primary antibodies used in the experiments were rabbit anti-pS10H3 and mouse anti-pS139H2AX (Millipore). Secondary antibodies

employed were goat anti-rabbit R-PE (Life Technologies), rabbit anti-mouse FITC (DAKO). Pacific Blue, Pacific Orange and FxCycle Far Red were obtained from Life Technologies. Hoechst 33358 was purchased from Calbiochem.

Staining, flow cytometry and microscopy

Cells were analyzed in an LSRII flow cytometer (Becton Dickinson). DNA content was measured by the integrated fluorescence intensity of Hoechst 33258 (1.5 μg/ml). Apoptotic cells were detected with the TUNEL assay (TdT-kit and Biotin-16-dUTP; Roche Diagnostics) as described earlier,[21] except that streptavidin-Cy5 (1:500) was used for detection. Mitotic cells were discriminated from interphase cells by staining with anti-phospho-S10-histone H3 (pS10H3; 1:500). DNA damage across the cell cycle was assessed by staining with anti-pS139H2AX (1:500). Appropriate fluorochrome-labeled anti-mouse/rabbit antibodies were used for detection of the primary ones and the cells were lastly stained for DNA content. The cells were blocked in 4% (w/v) nonfat dried milk during the staining with the respective primary and secondary antibodies. Doublets were discriminated from the analysis by using the area and width of the DNA staining signal. The gating structure used to obtain the flow cytometry results is shown in **Fig. S3**. Alternatively, Pacific Blue barcoding was used to compare levels of DNA damage (γH2AX) in samples treated with/without IR (i.e. in cases where the G_1 cells were not negative, see **Fig. 2A**). Cells were stained with Pacific Orange (20 min, 4°C, 0.475 ng/μl in PBS) for dead cell discrimination, and thereafter fixed. Fixed control cells were stained with Pacific Blue (15 min, RT, 0.015 ng/μl) and mixed with fixed treated cells. The mixed samples were thereafter stained for γH2AX, mitosis (as above), and DNA content with the FxCycle Far Red DNA stain (following the manufacturer's recommendation). Excitation wavelengths and emission filters used are listed in Fig. S1 in the accompanying article in this issue.

G_1, S, G_2H, G_2L and M cells were sorted using the regions shown in **Fig. S3**. Counting of γH2AX-foci in cells sorted by cell cycle-phase was performed with an Axio Z1 Imager microscope equipped with an ApoTome unit for optical sectioning, an AxioCam Mrm camera and Plan-Apochromat lenses (100x/NA1.40; 63x/NA1.40) (Carl Zeiss). Z-stacks with a distance of 1μm covering the complete depth of the cells were obtained. The gating strategy used to assess the cell cycle-resolved fractions of EdU-positive cells is also shown in **Fig. S3**.

Data treatment, statistical analysis, and simulation

The γH2AX focus count distributions could not be fitted with Poisson distributions for S, G_2 and G_2H, and were instead assumed to be normally distributed for statistical purposes. The distributions for the populations with low counts (G_1, G_2L and M) could likely have been fitted with Poisson distributions. Means and standard deviations are thus not well-defined for the latter 3, but we have still chosen to give these measures for all populations to illustrate the heterogeneity and to avoid the use of different statistical terms for the different populations.

The "robust coefficient of variation" (rCV) was calculated from the gated γH2AX distributions. The regions employed for gating were as shown in **Fig. S3**, except that there were no limitations on the γH2AX intensity for G_2. rCV is defined as: rCV (%) = 100 * ½ * (Intensity [at 84 percentile] - Intensity [at 16 percentile]) / Median.

There was a significant fraction of EdU^+ cells in G_2H and G_2L even at time zero after pulse labeling, less so in M and G_1 (**Fig. S4**). This was due to spillover of EdU^+ S phase cells into the regions employed for gating. This spillover was assumed to be constant up to 8 h, since the length of S phase in the cell lines employed here is longer than 8 h (Fig. S8 in the accompanying paper in this issue), and was used to obtain the corrected fractions shown in **Fig. 3** from the raw data shown in **Fig. S4**:

$$F_{corrected}(t) = \frac{F(t) - F(0)}{1 - F(0)}$$

where F(0) is the fraction of EdU^+ cells at time zero (spillover), and F(t) is the observed fraction of EdU^+ cells at time t.

The population of the subcompartments of G_2, and M, with EdU^+ cells emerging from S phase was simulated employing a model based on the experimental result that G_2H was populated before G_2L, the latter being populated before M (**Fig. 3**). For a (sub)phase that is directly fed from S phase (e.g. G_2H), the population (fraction of EdU^+ cells) in this phase at a time t after pulse labeling is described by:

$$F_D(t) = \frac{1}{\sum_{T=0}^{\infty} f(T) \times T} \sum_{T=0}^{\infty} f(T) \times T \times \left(\frac{t}{T}\right)$$

where $F_D(t)$ is the fraction of EdU^+ cells in the directly populated (sub)phase. t/T is set to 1 if t>T, and the summation runs from 0 to ∞ (in steps of 0.5 h, up to a maximum of 24 h in the attached program). f(T) describes the flux of cells into the compartments with different residence times in the directly populated phase. If e.g., the residence time T is equal for all cells, then f(T) is zero for all T's except the exact residence time where it is 1. If the residence time is heterogeneous, the (weighted) distribution f (T) may be specified in the attached program. This distribution is termed "flat" if the weight (amplitude) is constant for all residence times in a range. Notice that f(T) describes the flux out, as well as the flux into the subphase in the absence of cell death from this compartment. The weights entered in the attached program do not need to be normalized, as normalization is taken care of in the formula above and in the attached program.

The population of a (sub)phase of constant length (T_I) that is indirectly fed through another (e.g., G_2L through G_2H) of variable duration by EdU^+ cells is given by:

$$F_I(t) = \frac{1}{\sum_{T=0}^{\infty} f(T) \times T_I} \sum_{T=0}^{\infty} f(T) \times T_I \times \left(\frac{t-T}{T_I}\right)$$

where ($t-T/T_I$) is set to 0 if t <T, and to 1 if t-T> T_I. Notice that although non-zero amplitude for f(0) does not contribute when calculating $F_D(t)$, $F_I(t)$ will be affected. The amplitude f(0) describes the fraction of cells entering the "indirectly" populated

(sub)phase directly, and will be recognized as the fraction of cells leaving S phase with a low amount of damage, entering G_2L directly without spending time in G_2H.

Likewise, the population of a phase of constant length (T_{I2}) that is indirectly fed through 2 other (sub)phases (e.g., M through G_2H and G_2L) is described by:

$$F_{I2}(t) = \frac{1}{\sum_{T=8}^{\infty} f(T) \times T_{I2}} \sum_{T=0}^{\infty} f(T) \times T_{I2} \times \left(\frac{t - T - T_I}{T_{I2}} \right)$$

where T_{I2} is the residence time in the second indirectly populated phase (e.g., M, constant in attached program), and $((t-T-T_I)/T_{I2})$ is set to 0 if $t<T+T_I$, and to 1 if $t-T-T_I> T_{I2}$.

The algorithm for simulation of the population of the compartments with EdU^+ cells was written in Visual Basic 6.5 (Microsoft Corp.), and all input parameters were handled in the corresponding Excel worksheet (Supplemental File). These parameters included fixed G_2L (T_I) and M (T_{I2}) phase durations and a variable length of the G_2H compartment, described by f (T). Weighting of cells in the time intervals from minimum to maximum G_2H duration (with a time resolution of 30 minutes) is user-defined in the program. The algorithm assumed sequential entry of cells from the G_2H compartment into the 2 compartments with fixed durations (G_2L followed by M). A macro-activated Excel sheet containing the software is available ("H2AXCellCycleSupfile.xlsm"). Simulated G_2L, G_2H and M distributions were exported to, and plotted in Sigmaplot.

Disclosure of Potential Conflicts of Interest

No potential conflicts of interest were disclosed.

Acknowledgment

Lise Forfang kindly isolated and grew the primary B-lymphocytes.

Funding

We received grants from the Norwegian Cancer Society for this work.

Supplemental Material

Supplemental data for this article can be accessed on the publisher's website.

References

1. Pardee AB, James LJ. Selective killing of transformed baby hamster kidney (BHK) cells. Proc Natl Acad Sci U S A 1975; 72:4994-8; PMID:174089; http://dx.doi.org/10.1073/pnas.72.12.4994
2. Blagosklonny MV, Pardee AB. The restriction point of the cell cycle. Cell Cycle 2002; 1:103-10; PMID:12429916
3. Kastan MB, Onyekwere O, Sidransky D, Vogelstein B, Craig RW. Participation of p53 protein in the cellular response to DNA damage. Cancer Res 1991; 51:6304-11; PMID:1933891
4. Kuerbitz SJ, Plunkett BS, Walsh WV, Kastan MB. Wild-type p53 is a cell cycle checkpoint determinant following irradiation. Proc Natl Acad Sci U S A 1992; 89:7491-5; PMID:1323840; http://dx.doi.org/10.1073/pnas.89.16.7491
5. Damelin M, Bestor TH. The decatenation checkpoint. Br J Cancer 2007; 96:201-5; PMID:17211475; http://dx.doi.org/10.1038/sj.bjc.6603537
6. Baxter J. "Breaking Up Is Hard to Do": The formation and resolution of sister chromatid intertwines. J Mol Biol 2015; 427: 590-607.
7. Smits VA, Medema RH. Checking out the G(2)/M transition. Biochim Biophys Acta 2001; 1519:1-12; PMID:11406266; http://dx.doi.org/10.1016/S0167-4781(01)00204-4
8. Lukas J, Lukas C, Bartek J. Mammalian cell cycle checkpoints: signalling pathways and their organization in space and time. DNA Repair (Amst) 2004; 3:997-1007; PMID:15279786; http://dx.doi.org/10.1016/j.dnarep.2004.03.006
9. Larsson S, Ryden T, Holst U, Oredsson S, Johansson M. Estimating the distribution of the G(2) phase duration from flow cytometric histograms. Math Biosci 2008; 211:1-17; PMID:17942127; http://dx.doi.org/10.1016/j.mbs.2007.08.009
10. Zolzer F, Jagetia G, Streffer C. G2-block after irradiation of cells with different p53 status. Strahlenther Onkol 2014; 190:1075-9; PMID:24928247; http://dx.doi.org/10.1007/s00066-014-0690-5
11. Sorensen CS, Syljuasen RG, Falck J, Schroeder T, Ronnstrand L, Khanna KK, Zhou BB, Bartek J, Lukas J. Chk1 regulates the S phase checkpoint by coupling the physiological turnover and ionizing radiation-induced accelerated proteolysis of Cdc25A. Cancer Cell 2003; 3:247-58; PMID:12676583; http://dx.doi.org/10.1016/S1535-6108(03)00048-5
12. Sorensen CS, Syljuasen RG, Lukas J, Bartek J. ATR, Claspin and the Rad9-Rad1-Hus1 complex regulate Chk1 and Cdc25A in the absence of DNA damage. Cell Cycle 2004; 3:941-5; PMID:15190204; http://dx.doi.org/10.4161/cc.3.7.972
13. Huang X, Tanaka T, Kurose A, Traganos F, Darzynkiewicz Z. Constitutive histone H2AX phosphorylation on Ser-139 in cells untreated by genotoxic agents is cell-cycle phase specific and attenuated by scavenging reactive oxygen species. Int J Oncol 2006; 29:495-501; PMID:16820894
14. MacPhail SH, Banath JP, Yu Y, Chu E, Olive PL. Cell cycle-dependent expression of phosphorylated histone H2AX: reduced expression in unirradiated but not X-irradiated G1-phase cells. Radiat Res 2003; 159:759-67; PMID:12751958; http://dx.doi.org/10.1667/RR3003
15. Huang X, Halicka HD, Traganos F, Tanaka T, Kurose A, Darzynkiewicz Z. Cytometric assessment of DNA damage in relation to cell cycle phase and apoptosis. Cell Prolif 2005; 38:223-43; PMID:16098182; http://dx.doi.org/10.1111/j.1365-2184.2005.00344.x
16. Lobrich M, Shibata A, Beucher A, Fisher A, Ensminger M, Goodarzi AA, Barton O, Jeggo PA. gammaH2AX foci analysis for monitoring DNA double-strand break repair: strengths, limitations and optimization. Cell Cycle 2010; 9:662-9; PMID:20139725; http://dx.doi.org/10.4161/cc.9.4.10764
17. Ichijima Y, Sakasai R, Okita N, Asahina K, Mizutani S, Teraoka H. Phosphorylation of histone H2AX at M phase in human cells without DNA damage response. Biochem Biophys Res Commun 2005; 336:807-12; PMID:16153602; http://dx.doi.org/10.1016/j.bbrc.2005.08.164
18. McManus KJ, Hendzel MJ. ATM-dependent DNA damage-independent mitotic phosphorylation of H2AX in normally growing mammalian cells. Mol Biol Cell 2005; 16:5013-25; PMID:16030261; http://dx.doi.org/10.1091/mbc.E05-01-0065
19. Murai J, Huang SY, Das BB, Renaud A, Zhang Y, Doroshow JH, Ji J, Takeda S, Pommier Y. Trapping of PARP1 and PARP2 by Clinical PARP Inhibitors. Cancer Res 2012; 72:5588-99; PMID:23118055; http://dx.doi.org/10.1158/0008-5472.CAN-12-2753
20. Tkacz-Stachowska K, Lund-Andersen C, Velissarou A, Myklebust JH, Stokke T, Syljuasen RG. The amount of DNA damage needed to activate the radiation-induced G2 checkpoint varies between single cells. Radiother Oncol 2011; 101:24-7; PMID:21722983; http://dx.doi.org/10.1016/j.radonc.2011.05.060
21. Landsverk KS, Lyng H, Stokke T. The response of malignant B lymphocytes to ionizing radiation: cell cycle arrest, apoptosis and protection against the cytotoxic effects of the mitotic inhibitor nocodazole. Radiat Res 2004; 162:405-15; PMID:15447042; http://dx.doi.org/10.1667/RR3235